Variational Classification: A Probabilistic Generalization of the Softmax Classifier

Shehzaad Dhuliawala

shehzaad.dhuliawala@inf.ethz.ch

Department of Computer Science, ETH Zurich, Switzerland

Mrinmaya Sachan

mrin may a. sach an@inf.eth z.ch

Department of Computer Science, ETH Zurich, Switzerland

Carl Allen carl.allen@ai.ethz.ch

AI Centre, ETH Zurich, Switzerland

Abstract

We present a latent variable model for classification that provides a novel probabilistic interpretation of neural network softmax classifiers. We derive a variational training objective, analogous to the evidence lower bound (ELBO) used to train variational auto-encoders, that generalises the cross-entropy loss used to train classification models. Treating inputs to the softmax layer as samples of a latent variable, our abstracted perspective reveals a potential inconsistency between their anticipated distribution, required for accurate label predictions to be output, and their empirical distribution found in practice. We augment the variational objective to mitigate such inconsistency and encourage a chosen latent distribution, instead of the implicit assumption found in a standard softmax layer. Overall, we provide new theoretical insight into the inner workings of widely-used softmax classifiers. Empirical evaluation on image and text classification datasets demonstrates that our proposed approach, $variational\ classification^1$, maintains classification accuracy while the reshaped latent space improves other desirable properties of a classifier, such as calibration, adversarial robustness, robustness to distribution shift and sample efficiency useful in low data settings.

1 Introduction

Classification is a central task in machine learning, used to categorise objects (Klasson et al., 2019), provide medical diagnoses (Adem et al., 2019; Mirbabaie et al., 2021), or identify potentially life-supporting planets (Tiensuu et al., 2019). Classification also arises in other learning regimes, e.g. to select actions in reinforcement learning, distinguish positive and negative samples in contrastive learning, and pertains to the attention mechanism in transformer models (Vaswani et al., 2017). Classification is commonly tackled by training a neural network with a sigmoid or softmax output layer.² Each data sample x is mapped deterministically by an encoder f_{ω} (with weights ω) to a real vector $z = f_{\omega}(x)$, which the softmax layer maps to a distribution over class labels $y \in \mathcal{Y}$:

 $p_{\theta}(y|x) = \frac{\exp\{z^{\top}w_y + b_y\}}{\sum_{y' \in \mathcal{Y}} \exp\{z^{\top}w_{y'} + b_{y'}\}}.$ (1)

Softmax classifiers have achieved impressive performance (e.g. Krizhevsky et al., 2012), however they are known to suffer from several issues. For example: such classifiers are trained to numerically minimise a loss function over a random dataset and their resulting predictions are hard to explain; model predictions may accurately identify the correct class by their mode but less accurately reflect a meaningful class distribution p(y|x), known as miscalibration; predictions can vary materially and erroneously for imperceptible changes in the data (adversarial examples); and highly flexible neural networks are often used in order to achieve accurate predictions, which tend to require considerable labelled data to train.

 $^{^{1}\}mathrm{Code}$: www.github.com/shehzaadzd/variational-classification. Review: www.openreview.net/forum?id=EWv9XGOpB3

²We refer throughout to the softmax function since it generalises sigmoid to multiple classes, but arguments apply to both.

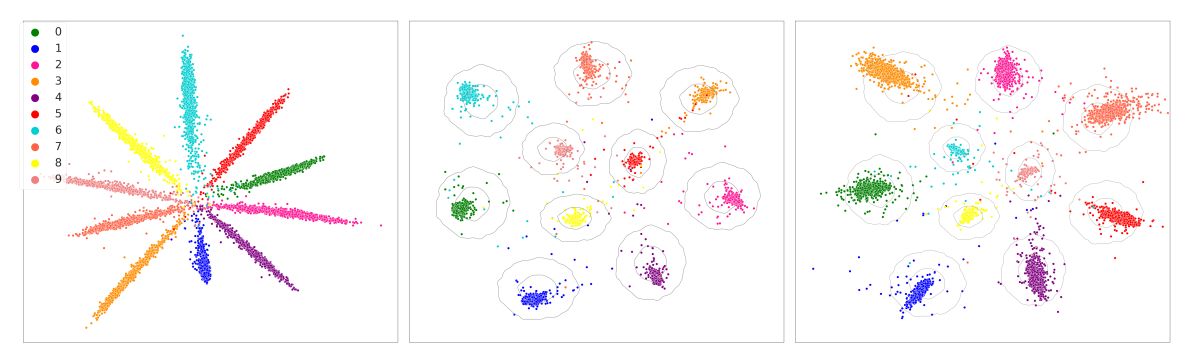


Figure 1: Empirical distributions of inputs to the output layer $q_{\phi}(z|y)$ for classifiers trained under incremental components of the VC objective (Eqn. 7) on MNIST (cf the central \mathcal{Z} -plane in figure 2). (l) "MLE" objective = softmax cross-entropy; (c) "MAP" objective = MLE + Gaussian class priors $p_{\theta}(z|y)$ (in contour); (r) VC objective = MAP + entropy of $p_{\theta}(z|y)$. Colour indicates class y; $\mathcal{Z} = \mathbb{R}^2$ for visualisation purposes.

In order to better understand softmax classification and ideally mitigate some of its known shortcomings, we take a latent perspective, introducing a latent variable z in a graphical (Markov) model $y \to z \to x$. This model can be interpreted generatively as first choosing a sample's class, or what it is (y); then parameters defining its attributes, e.g. size, colour (z); which determine the observation (x), subject to any stochasticity, e.g. noise or natural variation. Class labels can be inferred by learning to reverse the process: predicting z from x, and y from z, integrating over all z: $p_{\theta,\phi}(y|x) = \int_z p_{\theta}(y|z)q_{\phi}(z|x)$. It is generally intractable to learn parameters (θ,ϕ) of this predictive model by maximising the log likelihood, $\int_{x,y} p(x,y) \log p_{\theta,\phi}(y|x)$. Instead a lower bound on the log likelihood can be maximised, comparable to the evidence lower bound (ELBO) used to train a variational auto-encoder (VAE) (Kingma & Welling, 2014; Rezende et al., 2014).

We show that training a softmax classifier under cross entropy loss (SCE) is, in fact, a special case of training this generalised latent classification model under the variational objective, in which the input to the softmax layer (z of Eqn. 1) is treated as the latent variable, the encoder parameterises $q_{\phi}(z|x)$, and the softmax layer computes $p_{\theta}(y|z)$. In other words, the latent variable model and its training objective provide an interpretable generalisation of softmax classification. Probing further, the softmax layer can be interpreted as applying Bayes' rule, $p_{\theta}(y|z) = \frac{p_{\theta}(z|y)p_{\theta}(y)}{\sum_{y'} p_{\theta}(z|y')p_{\theta}(y')}$, assuming that latent variables follow exponential family class-conditional distributions $p_{\theta}(\mathbf{z}|\mathbf{y})$ for true class distributions to be output. Meanwhile, the distribution that latents actually follow, $q_{\phi}(\mathbf{z}|y) = \int_{x} q_{\phi}(\mathbf{z}|x)p(x|y)$, is defined by the data distribution and the encoder. We refer to these two descriptions of p(z|y) as the anticipated and empirical latent distributions, respectively, and consider their relationship. We show, both theoretically and empirically, that in practical settings these distributions can materially differ. Indeed, optimising the SCE objective may cause each empirical distribution $q_{\phi}(z|y)$ to collapse to a point rather than fit the anticipated $p_{\theta}(z|y)$. This essentially overfits to the data and loses information required for estimating confidence or other potential downstream tasks, limiting the use of z as a representation of x. To address the potential discrepancy between $q_{\phi}(\mathbf{z}|y)$ and $p_{\theta}(\mathbf{z}|y)$, so that the softmax layer receives the distribution it expects, we minimise the Kullback-Leibler (KL) divergence between them. This is non-trivial since $q_{\phi}(\mathbf{z}|\mathbf{y})$ can only be sampled not evaluated, hence we use the density ratio trick (Nguyen et al., 2010; Gutmann & Hyvärinen, 2010), as seen elsewhere (Makhzani et al., 2015; Mescheder et al., 2017), to approximate the required log probability ratios as an auxiliary task.

The resulting Variational Classification (VC) objective generalises softmax cross-entropy classification from a latent perspective and fits empirical latent distributions $q_{\phi}(\mathbf{z}|y)$ to anticipated class priors $p_{\theta}(\mathbf{z}|y)$. Within this more interpretable framework, latent variables learned by a typical softmax classifier can be considered maximium likelihood (MLE) point estimates that maximise $p_{\theta}(y|z)$. By comparison, the two KL components introduced in variational classification, respectively lead to maximum a posteriori (MAP) point estimates; and a Bayesian treatment where latent variables (approximately) fit the full distribution $p_{\theta}(\mathbf{z}|y)$ (Figure 1).⁴ Since Variational Classification serves to mitigate over-fitting, which naturally reduces with increased samples, VC is anticipated to offer greatest benefit in low data regimes.

³We use the notation q_{ϕ} to distinguish distributions, as will be made clear.

⁴Terms of the standard ELBO can be interpreted similarly.

Through a series of experiments on vision and text datasets, we demonstrate that VC achieves comparable accuracy to regular softmax classification while the aligned latent distribution improves calibration, robustness to adversarial perturbations (specifically FGSM "white box"), generalisation under domain shift and performance in low data regimes. Although many prior works target any *one* of these pitfalls of softmax classification, often requiring extra hyperparameters to be tuned on held-out validation sets, VC *simultaneously improves them all*, without being tailored towards any or needing further hyperparameters or validation data. Overall, the VC framework gives novel mathematical insight and interpretability to softmax classification: the encoder maps a mixture of unknown data distributions p(x|y) to a mixture of chosen latent distributions p(x|y), which the softmax/output layer "flips" by Bayes' rule. This understanding may enable principled improvement of classification and its integration with other latent variable paradigms (e.g. VAEs).

2 Background

The proposed generalisation from softmax to variational classification (§3) is analogous to how a deterministic auto-encoder relates to a *variational auto-encoder* (VAE), as briefly summarised below.

Estimating parameters of a latent variable model of the data $p_{\theta}(x) = \int_{z} p_{\theta}(x|z) p_{\theta}(z)$ by maximising the likelihood, $\int_{x} p(x) \log p_{\theta}(x)$, is often intractable. Instead, one can maximise the *evidence lower bound* (ELBO):

$$\int_{x} p(x) \log p_{\theta}(x) = \int_{x} p(x) \int_{z} q_{\phi}(z|x) \left\{ \log p_{\theta}(x|z) - \log \frac{q_{\phi}(z|x)}{p_{\theta}(z)} + \log \frac{q_{\phi}(z|x)}{p_{\theta}(z|x)} \right\}$$

$$\geq \int_{x} p(x) \int_{z} q_{\phi}(z|x) \left\{ \log p_{\theta}(x|z) - \log \frac{q_{\phi}(z|x)}{p_{\theta}(z)} \right\} \stackrel{.}{=} \mathbf{ELBO}, \tag{2}$$

where $q_{\phi}(z|x)$ is the approximate posterior and the term dropped in the inequality is a Kullback-Leibler (KL) divergence, $D_{\text{KL}}[q(z)||p(z)] \doteq \int_{z} q(z) \log \frac{q(z)}{p(z)} \geq 0$. The VAE (Kingma & Welling, 2014; Rezende et al., 2014) uses the ELBO as a training objective with $p_{\theta}(x|z)$ and $q_{\phi}(z|x)$ assumed to be Gaussian parameterised by neural networks. Setting the variance of $q_{\phi}(z|x)$ to zero, i.e. each $q_{\phi}(z|x)$ to a delta distribution, the first ("reconstruction") term of Eqn. 2 equates to the training objective of a deterministic auto-encoder, which the VAE can be interpreted to probabilistically generalise, allowing for uncertainty or stochasticity in $q_{\phi}(z|x)$ constrained by the second ("regularisation") term.

Maximising the ELBO directly equates to minimising $D_{\text{KL}}[p(x)||p_{\theta}(x)] + \mathbb{E}_x[D_{\text{KL}}[q_{\phi}(z|x)||p_{\theta}(z|x)]]$, and so fits the model $p_{\theta}(x)$ to the data distribution p(x) and $q_{\phi}(z|x)$ to the model posterior $p_{\theta}(z|x) \doteq \frac{p_{\theta}(x|z)p_{\theta}(z)}{p_{\theta}(x)}$. Equivalently, the modelled distributions $q_{\phi}(z|x)$ and $p_{\theta}(x|z)$ are made consistent under Bayes' rule.

3 Variational Classification

Classification Latent Variable Model (LVM): Consider data $x \in \mathcal{X}$ and labels $y \in \mathcal{Y}$ as samples of random variables x, y jointly distributed p(x, y). Under the (Markov) generative model in Figure 2 (*left*),

$$p(x) = \int_{y,z} p(x|z)p(z|y)p(y) , \qquad (3)$$

labels can be predicted by reversing the process,

$$p_{\theta}(y|x) = \int_{z} p_{\theta}(y|z) p_{\theta}(z|x) . \tag{4}$$

A neural network (NN) softmax classifier is a deterministic function that maps each data point x, via a sequence of intermediate representations, to a point on

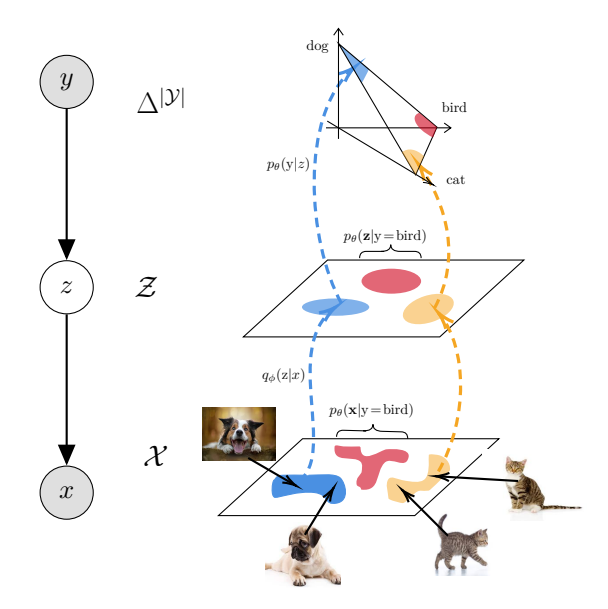


Figure 2: Variational Classification, reversing the generative process: $q_{\phi}(\mathbf{z}|x)$ maps data $x \in \mathcal{X}$ to the latent space \mathcal{Z} , where *empirical* distributions $q_{\phi}(\mathbf{z}|y)$ are fitted to *class priors* $p_{\theta}(\mathbf{z}|y)$; top layer computes $p_{\theta}(y|z)$ by Bayes' rule to give a class prediction p(y|x).

the simplex $\Delta^{|\mathcal{Y}|}$ that parameterises a categorical label distribution $p_{\theta}(y|x)$. Any intermediate representation z = q(x) can be considered a sample of a *latent* random variable z from conditional distribution $p(z|x) = \delta_{z-g(x)}$.

Proposition: a NN softmax classifier is a special case of Eqn. 4.

Proof: Define (i) the input to the softmax layer as latent variable z; (ii) $p_{\theta}(z|x) = \delta_{z-f_{\omega}(x)}$, a delta distribution parameterised by f_{ω} , the NN up to the softmax layer (the encoder); and (iii) $p_{\theta}(y|z)$ by the softmax layer (as defined in RHS of Eqn. 1).

Training a Classification LVM 3.1

Similarly to the latent variable model for $p_{\theta}(x)$ (§2), parameters of Eqn. 4 cannot in general be learned by directly maximising the likelihood. Instead we can maximise a lower bound:

$$\int_{x,y} p(x,y) \log p_{\theta}(y|x) = \int_{x,y} p(x,y) \int_{z} q_{\phi}(z|x) \left\{ \log p_{\theta}(y|z, \mathbf{x}) - \frac{\log \frac{q_{\phi}(z|x)}{p_{\theta}(z|x)}}{p_{\theta}(z|x)} + \log \frac{q_{\phi}(z|x)}{p_{\theta}(z|x,y)} \right\}$$

$$\geq \int_{x,y} p(x,y) \int_{z} q_{\phi}(z|x) \log p_{\theta}(y|z) \doteq \mathbf{ELBO_{VC}} \tag{5}$$

Here, $p_{\theta}(y|z,x) = p_{\theta}(y|z)$ by the Markov model, and the (freely chosen) variational posterior q_{ϕ} is assumed to depend only on x and set equal to $p_{\theta}(z|x)$ (eliminating the second term).⁵ The derivation of Eqn. 5 follows analogously to that of Eqn. 2 conditioned on x; an alternative derivation follows from Jensen's inequality.

Unlike for the standard ELBO, the "dropped" KL term $D_{\text{KL}}[q_{\phi}(z|x) || p_{\theta}(z|x,y)]$ (minimised implicitly as ELBO_{VC} is maximised) may not minimise to zero – except in the limiting case $p_{\theta}(y|x,z) = p_{\theta}(y|z)$. That is, when z is a sufficient statistic for y given x, intuitively meaning that z contains all information contained in x about y. Hence, maximising ELBO_{VC} implicitly encourages z to learn a sufficient statistic for y|x.

Proposition: softmax cross-entropy (SCE) loss is a special case of ELBO_{VC}.

Proof: In Eqn. 5, let (i) $q_{\phi}(z|x) = \delta_{z-f_{\omega}(x)}$; and (ii) $p_{\theta}(z|y) = h(z) \exp\{z^{\top}w_y + b'_y\}, \forall y \in \mathcal{Y}$, for constants w_y, b'_y , arbitrary positive function $h: \mathcal{Z} \to \mathbb{R}^+$ and $b_y = b'_y + \log p_{\theta}(y)$:

$$\int_{x,y} p(x,y) \int_{z} q_{\phi}(z|x) \log p_{\theta}(y|z) \stackrel{(i)}{=} \int_{x,y} p(x,y) \log p_{\theta}(y|z=f_{\omega}(x)) \stackrel{(Bayes)}{=} \int_{x,y} p(x,y) \log \frac{p_{\theta}(z=f_{\omega}(x)|y)p_{\theta}(y)}{\sum_{y'} p_{\theta}(z=f_{\omega}(x)|y')p_{\theta}(y')}$$

$$\stackrel{(ii)}{=} \int_{x,y} p(x,y) \log \frac{p_{\theta}(z) \exp\{f_{\omega}(x) + g_{\theta}(x) + g_{$$

Corollary: A NN softmax classifier outputs true label distributions p(y|x) if inputs to the softmax layer, z, follow anticipated class-conditional distributions $p_{\theta}(z|y)$ of (equi-scale) exponential family form.

3.2 Anticipated vs Empirical Latent Distributions

Defining an LVM for classification (Eqn. 4) requires specifying $p_{\theta}(y|z)$. In the special case of softmax classification, $p_{\theta}(y|z)$ is effectively encoded by Bayes' rule assuming exponential family $p_{\theta}(z|y)$, i.e. distributions over softmax layer inputs for class y (Eqn. 6). More generally, one can choose the parametric form of $p_{\theta}(z|y)$ and compute $p_{\theta}(y|z)$ by Bayes' rule in a classifier's output layer (generalising the standard softmax layer), thereby encoding the distribution latent variables are anticipated to follow for accurate label predictions p(y|x) to be output. A natural question then is: do latent variables of a classification LVM empirically follow the **anticipated** distributions $p_{\theta}(z|y)$?

Empirical latent distributions are not fixed, but rather defined by $q_{\phi}(z|y) = \int_{x} q_{\phi}(z|x)p(x|y)$, i.e. by sampling $q_{\phi}(z|x)$ (parameterised by the encoder f_{ω}) given class samples $x \sim p(x|y)$. Since ELBO_{VC} is optimised w.r.t. parameters ϕ , if optimal parameters are denoted ϕ^* , the question becomes: does $q_{\phi^*}(z|y) = p_{\theta}(z|y)$?

It can be seen that ELBO_{VC} is optimised w.r.t ϕ if $q_{\phi^*}(z|x) = \delta_{z-z_x}$, for $z_x = \arg\max_z \mathbb{E}_{y|x}[\log p_{\theta}(y|z)]$ (see appendix A.1). In practice, true label distributions p(y|x) are unknown and we have only finite samples

⁵We use the notation " q_{ϕ} " by analogy to the VAE and to later distinguish $q_{\phi}(z|y)$, derived from $q_{\phi}(z|x)$, from $p_{\theta}(z|y)$.

⁶Proof: from p(z|x,y)p(y|x) = p(y|x,z)p(z|x) and Markovianity, we see that $D_{\text{KL}}[q_{\phi}(z|x)||p_{\theta}(z|x,y)] = 0 \Leftrightarrow p_{\theta}(z|x,y) = 0$ $q_{\phi}(z|x) \Leftrightarrow p_{\theta}(y|x) = p_{\theta}(y|x,z) = p_{\theta}(y|z) \Leftrightarrow \text{z a sufficient statistic for y}|x.$ The assume the parametric family q_{ϕ} is sufficiently flexible to closely approximate the analytic maximiser of ELBO_{VC}.

from them. For a continuous data domain \mathcal{X} , e.g. images or sounds, any empirically observed x is sampled twice with probability zero and so is observed once with a single label y(x). A similar situation arises (for any \mathcal{X}) if – as a property of the data – every x has only one ground truth label y(x), i.e. labels are mutually exclusive and partition the data.⁸ In either case, the expectation over labels simplifies and, for a given class y, $z_x = \arg \max_z p_{\theta}(y(x)|z)$, meaning the optimal latent distribution $q_{\phi^*}(z|x)$ is identical for all samples x of class y. Letting z_y denote the optimal latent variable for all x of class y, optimal class-level distributions are simply $q_{\phi^*}(z|y) = \delta_{z-z_y}$, and ELBO_{VC} is maximised if all representations of class y, defined by $q_{\phi}(z|y)$, "collapse" to the same point, a distribution that may differ materially to anticipated $p_{\theta}(z|y)$.

Since softmax classification is a special case, this reveals the potential for softmax classifiers to learn over-concentrated, or over-confident, latent distributions relative to anticipated distributions (subject to the data distribution and model flexibility). In practical terms, the softmax cross-entropy loss may be minimised when all samples of a given class are mapped (by the encoder f_{ω}) to the same latent variable/representation, regardless of differences in the samples' probabilities or semantics, thus disregarding information that may be useful for calibration or downstream tasks. We note that the Information Bottleneck Theory (Tishby et al., 2000; Tishby & Zaslavsky, 2015; Shwartz-Ziv & Tishby, 2017) presumes that such "loss of information" is beneficial, but as we see below, not only is it unnecessary for classification, it may be undesirable in general.

3.2.1 Aligning the Anticipated and Empirical Latent Distributions

We have shown that the ELBO_{VC} objective, a generalisation of SCE loss, effectively involves two versions of the latent class conditional distributions, $p_{\theta}(z|y)$ and $q_{\phi}(z|y)$, and that a mismatch between them may have undesirable consequences in terms of information loss. We therefore propose to align $p_{\theta}(z|y)$ and $q_{\phi}(z|y)$, or, equivalently, for $p_{\theta}(y|z)$ and $q_{\phi}(z|y)$ to be made consistent under Bayes' rule (analogous to $p_{\theta}(x|z)$ and $q_{\phi}(z|x)$ in the ELBO, §2). Specifically, we minimise $D_{\text{KL}}[q_{\phi}(z|y)||p_{\theta}(z|y)]$, $\forall y \in \mathcal{Y}$. Including this constraint (weighted by $\beta > 0$) and learning required class distribution $p_{\pi}(y)$ defines the full **VC objective**

$$-\mathcal{L}_{\mathbf{VC}} = \int_{x,y} p(x,y) \left\{ \int_{z} q_{\phi}(z|x) \log \frac{p_{\theta}(z|y)p_{\pi}(y)}{\sum_{y'} p_{\theta}(z|y')p_{\pi}(y')} - \beta \int_{z} q_{\phi}(z|y) \log \frac{q_{\phi}(z|y)}{p_{\theta}(z|y)} + \log p_{\pi}(y) \right\}.$$
 (7)

Taken incrementally, q_{ϕ} -terms of \mathcal{L}_{VC} can be interpreted as treating the latent variable z from a maximum likelihood (MLE), maximum a posteriori (MAP) and Bayesian perspective:

(i) maximising
$$\int_{z} q_{\phi}(z|x) \log p_{\theta}(y|z)$$
 may overfit $q_{\phi}(z|y) \approx \delta_{z-z_{\eta}}$ (as above); [MLE]

(ii) adding class priors
$$\int_z q_{\phi}(z|y) \log p_{\theta}(z|y)$$
 changes the point estimates z_y ; [MAP]

(iii) adding
$$entropy = -\int_{z} q_{\phi}(z|y) \log q_{\phi}(z|y)$$
 encourages $q_{\phi}(z|y)$ to "fill out" $p_{\theta}(z|y)$. [Bayesian]

Figure 1 shows samples from empirical latent distributions $q_{\phi}(\mathbf{z}|y)$ for classifiers trained under incremental terms of the VC objective. This empirically confirms that softmax cross-entropy loss does not impose the anticipated latent distribution encoded in the output layer (left). Adding class priors $p_{\theta}(\mathbf{z}|y)$ changes the point at which latents of a class concentrate (centre). Adding entropy encourages class priors to be "filled out" (right), relative to previous point estimates/ δ -distributions. As above, if each x has a single label (e.g. MNIST), the MLE/MAP training objectives are optimised when class distributions $q_{\phi}(\mathbf{z}|y)$ collapse to a point. We note that complete collapse is not observed in practice (Figure 1, left, centre), which we conjecture is due to strong constraints on f_{ω} , in particular continuity, ℓ_2 regularisation and early stopping based on validation loss. Compared to the KL form of the ELBO (§2), maximising Eqn. 7 is equivalent to minimising:

$$\mathbb{E}_{x}\left[D_{\mathrm{KL}}\left[p(y|x)\|p_{\theta}(y|x)\right] + \mathbb{E}_{x,y}\left[D_{\mathrm{KL}}\left[q_{\phi}(z|x)\|p_{\theta}(z|x,y)\right]\right] + \mathbb{E}_{y}\left[D_{\mathrm{KL}}\left[q_{\phi}(z|y)\|p_{\theta}(z|y)\right]\right] + D_{\mathrm{KL}}\left[p(y)\|p_{\pi}(y)\right]\right] \tag{8}$$

showing the extra constraints over the core objective of modelling p(y|x) with $p_{\theta}(y|x)$ (underlined).

⁸As in popular image datasets, e.g. MNIST, CIFAR, ImageNet, where samples belong to one class or another.

⁹Subject to uniqueness of $\arg\max_z p_\theta(y|z)$, which is not guaranteed in general, but is assumed for suitable $p_\theta(z|y)$, such as the softmax case of central interest: if all x have a single label y(x) (i.e. $p(y|x) = \mathbf{1}_{y=y(x)}$ is a "one-hot" vector), and norms are finitely constrained ($||z|| = \alpha > 0$), then the SCE objective (Eqn. 6) is maximised, and softmax outputs $p_\theta(y|x)$ (Eqn. 1) increasingly approximate true p(y|x), as class parameters w_y are maximally dispersed (i.e. unit vectors \hat{w}_y tend to a regular polytope on the unit sphere) and all representations of a class y align with the class parameter: $z_x = f_\omega(x) \to \alpha \hat{w}_{y(x)}$ (unique).

Algorithm 1 Variational Classification (VC)

```
1: Input p_{\theta}(\mathbf{z}|\mathbf{y}), q_{\phi}(\mathbf{z}|\mathbf{x}), p_{\pi}(\mathbf{y}), T_{\psi}(z); learning rate schedule \{\eta^t_{\theta}, \eta^t_{\tau}, \eta^t_{\tau}, \eta^t_{\psi}\}_t, \beta

2: Initialise \theta, \phi, \pi, \psi; t \leftarrow 0

3: while not converged do

4: \{x_i, y_i\}_{i=1}^m \sim \mathcal{D} [sample batch from data distribution p(\mathbf{x}, \mathbf{y})]

5: for \mathbf{z} = \{1 \dots \mathbf{m}\} do

6: z_i \sim q_{\phi}(\mathbf{z}|x_i), z_i' \sim p_{\theta}(\mathbf{z}|y_i) [e.g. q_{\phi}(\mathbf{z}|x_i) = \delta_{z-f_{\omega}(x_i)}, \phi = \omega \Rightarrow z_i = f_{\omega}(x_i)]

7: p_{\theta}(y_i|z_i) = \sum_{y \theta(z_i|y_i)p_{\pi}(y_i)}^{p_{\theta}(z_i|y_i)p_{\pi}(y)}

8: end for

9: g_{\theta} \leftarrow \frac{1}{m} \sum_{i=1}^m \nabla_{\theta} [\log p_{\theta}(y_i|z_i) + \beta p_{\theta}(z_i|y_i)]

10: g_{\phi} \leftarrow \frac{1}{m} \sum_{i=1}^m \nabla_{\phi} [\log p_{\theta}(y_i|z_i) - \beta T_{\psi}(z_i)] [e.g. using "reparameterisation trick"]

11: g_{\pi} \leftarrow \frac{1}{m} \sum_{i=1}^m \nabla_{\pi} \log p_{\pi}(y_i)

12: g_{\psi} \leftarrow \frac{1}{m} \sum_{i=1}^m \nabla_{\psi} [\log \sigma(T_{\psi}(z_i)) + \log(1 - \sigma(T_{\psi}(z_i'))]

13: \theta \leftarrow \theta + \eta^t_{\theta} g_{\theta}, \quad \phi \leftarrow \phi + \eta^t_{\phi} g_{\phi}, \quad \pi \leftarrow \pi + \eta^t_{\pi} g_{\pi}, \quad \psi \leftarrow \psi + \eta^t_{\psi} g_{\psi}, \quad t \leftarrow t + 1

14: end while
```

3.3 Optimising the VC Objective

The VC objective (Eqn. 7) is a lower bound that can be maximised by gradient methods, e.g. SGD:

- the first term can be calculated by sampling $q_{\phi}(\mathbf{z}|x)$ (using the "reparameterisation trick" as necessary (Kingma & Welling, 2014)) and computing $p_{\theta}(\mathbf{y}|\mathbf{z})$ by Bayes' rule;
- the third term is standard multinomial cross-entropy;
- the second term, however, is not readily computable since $q_{\phi}(\mathbf{z}|y)$ is implicit and cannot easily be evaluated, only sampled, as $z \sim q_{\phi}(\mathbf{z}|x)$ (parameterised by f_{ω}) for class samples $x \sim p(\mathbf{x}|y)$.

Fortunately, we require log ratios $\log \frac{q_{\phi}(z|y)}{p_{\theta}(z|y)}$ for each class y, which can be approximated by training a binary classifiers to distinguish samples of $q_{\phi}(z|y)$ from those of $p_{\theta}(z|y)$. This so-called *density ratio trick* underpins learning methods such as Noise Contrastive Estimation (Gutmann & Hyvärinen, 2010) and contrastive self-supervised learning (e.g. Oord et al., 2018; Chen et al., 2020) and has been used comparably to train variants of the VAE (Makhzani et al., 2015; Mescheder et al., 2017).

Specifically, we maximise the following auxiliary objective w.r.t. parameters ψ of a set of binary classifiers:

$$-\mathcal{L}_{\mathbf{aux}} = \int_{\mathcal{U}} p(y) \left\{ \int_{z} q_{\phi}(z|y) \log \sigma(T_{\psi}^{y}(z)) + \int_{z} p_{\theta}(z|y) \log(1 - \sigma(T_{\psi}^{y}(z))) \right\}$$
(9)

where σ is the logistic sigmoid function $\sigma(x) = (1 + e^{-x})^{-1}$, $T_{\psi}^{y}(z) = w_{\psi}^{\top} z + b_{y}$ and $\psi = \{w_{y}, b_{y}\}_{y \in \mathcal{Y}}$.

It is easy to show that Eqn. 9 is optimised if $T_{\psi}^{y}(z) = \log \frac{q_{\phi}(z|y)}{p_{\theta}(z|y)}$, $\forall y \in \mathcal{Y}$. Hence, when all binary classifiers are trained, $T_{\psi}^{y}(z)$ approximates the log ratio for class y required by the VC objective (Eqn. 7). Optimising the VC objective might, in principle, also require gradients of the approximated log ratios w.r.t. parameters θ and ϕ . However, the gradient w.r.t. the ϕ found within the log ratio is always zero (Mescheder et al., 2017) and so the gradient w.r.t. θ can be computed from Eqn. 7. See Algorithm 1 for a summary.

This approach is adversarial since (a) the VC objective is maximised when log ratios give a minimal KL divergence, i.e. when $q_{\phi}(z|y) = p_{\theta}(z|y)$ and latents sampled from $q_{\phi}(z|y)$ or $p_{\theta}(z|y)$ are indistinguishable; whereas (b) the auxiliary objective is maximised if the ratios are maximal and the two distributions are fully discriminated. Relating to a Generative Adversarial Network (GAN) (Goodfellow et al., 2014a), the encoder f_{ω} acts as a generator and each binary classifier as a discriminator. Unlike a GAN, VC requires a discriminator per class that each distinguish generated samples from a learned, rather than static, reference/noise distribution $p_{\theta}(z|y)$. However, whereas a GAN discriminator distinguishes between complex distributions in the data domain, a VC discriminator compares a Gaussian to an approximate Gaussian in the lower dimensional latent domain, a far simpler task. The auxiliary objective does not change the complexity relative to softmax classification and can be parallelised across classes, adding marginal computational overhead per class.

3.3.1 Optimum of the VC Objective

In §3.2, we showed that the empirical distribution $q_{\phi}(z|x)$ that opitimises the ELBO_{VC} need not match the anticipated $p_{\theta}(z|y)$. Here, we perform similar analysis to identify $q_{\phi^*}(z|x)$ that maximises the VC objective, which, by construction of the objective, is expected to better match the anticipated distribution.

Letting $\beta = 1$ to simplify (see appendix A.2 for general case), the VC objective is maximised w.r.t. $q_{\phi}(z|x)$ if:

$$\mathbb{E}_{p(y|x)}[\log q_{\phi}(z|y)] = \mathbb{E}_{p(y|x)}[\log p_{\theta}(y|z)p_{\theta}(z|y)] + c , \qquad (10)$$

for a constant c. This is satisfied if, for each class y,

$$q_{\phi}(z|y) = p_{\theta}(z|y) \frac{p_{\theta}(y|z)}{\mathbb{E}_{p_{\theta}(z'|y)}[p_{\theta}(y|z')]} , \qquad (11)$$

giving a unique solution if each x has a single label y (see §3.2; see appendix A.2 for proof). This shows that each $q_{\phi}(z|y)$ fits $p_{\theta}(z|y)$ scaled by a ratio of $p_{\theta}(y|z)$ to its weighted average. Hence, where $p_{\theta}(y|z)$ is above average, $q_{\phi}(z|y) > p_{\theta}(z|y)$, and vice versa. In simple terms, $q_{\phi}(z|y)$ reflects $p_{\theta}(z|y)$ but is "peakier" (fitting observation in Figure 1). We have thus shown empirically (Figure 1) and theoretically that the VC objective aligns the empirical and anticipated latent distributions. However, these distributions are not identical and we leave to future work the derivation of an objective that achieves both $p_{\theta}(y|x) = p(y|x)$ and $q_{\phi}(z|y) = p_{\theta}(z|y)$.

3.4 Summary

The latent variable model for classification (Eqn. 4) abstracts a typical softmax classifier, giving interpretability to its components:

- the encoder (f_{ω}) transforms a mixture of analytically unknown class-conditional data distributions $p(\mathbf{x}|y)$ to a mixture of analytically defined latent distributions $p_{\theta}(\mathbf{z}|y)$;
- assuming latent variables follow the anticipated class distributions $p_{\theta}(\mathbf{z}|\mathbf{y})$, the output layer applies Bayes' rule to give $p_{\theta}(\mathbf{y}|\mathbf{z})$ (see figure 2) and thus meaningful estimates of label distributions $p(\mathbf{y}|\mathbf{x})$ (by Eqn. 4).

ELBO_{VC} generalises softmax cross-entropy, treating the input to the softmax layer as a latent variable and identifying the anticipated class-conditionals $p_{\theta}(z|y)$ implicitly encoded within the softmax layer. Extending this, the VC objective (\mathcal{L}_{VC}) encourages the empirical latent distributions $q_{\phi}(z|y)$ to fit $p_{\theta}(z|y)$. Softmax cross-entropy loss is recovered from \mathcal{L}_{VC} by setting (i) $q_{\phi}(z|x) = \delta_{z-f_{\omega}(x)}$; (ii) $p_{\theta}(z|y)$ to (equal-scale) exponential family distributions, e.g. equivariate Gaussians; and (iii) $\beta = 0$. This is analogous to how a deterministic auto-encoder relates to a VAE. Thus the VC framework elucidates assumptions made implicitly in softmax classification and by generalising this special case, allows these assumptions, e.g. the choice of $p_{\theta}(z|y)$, to be revised on a task/data-specific basis.

4 Related Work

Despite notable differences, the *energy-based* interpretation of softmax classification of Grathwohl et al. (2019) is perhaps most comparable to our own in taking an abstract view to improve softmax classification. However, their gains, e.g. in calibration and adversarial robustness, come at a significant cost to the main aim: classification accuracy. Further, the required MCMC normalisation reportedly slows and destabilises training. In contrast, we use tractable probability distributions and retain the order of complexity. Our approach is also notionally related to Bayesian Neural Networks (BNNs) or related approaches such as MC-dropout (Gal & Ghahramani, 2016), although these are *Bayesian* with respect to model parameters, rather than latent variables. In principle, these might be combined (e.g. Murphy, 2012) as an interesting future direction.

Several previous works adapt the standard ELBO for learning a model of p(x), to a conditional analog for learning p(y|x) (Tang & Salakhutdinov, 2013; Sohn et al., 2015). However, such works focus on generative scenarios rather than discriminative classification, e.g. x being a face image and y|x being the same face in a different pose determined by latent z; or x being part of an image and y|x being its completion given latent content z. The Gaussian stochastic neural network (GSNN) model (Sohn et al., 2015) is closer to our own by conditioning q(z|x,y) only on x, however the model neither generalises softmax classification nor considers class-level latent priors q(z|y) as in variational classification.

Variational classification subsumes a number of works that add a regularisation term to the softmax crossentropy loss function, which can be interpreted as a *prior* over latent variables in the "MAP" case (§3.2.1). For example, several semi-supervised learning models can be interpreted as treating softmax *outputs*, i.e. class predictions, as latent variables and adding a latent prior to "guide" predictions of unlabelled data (Allen et al., 2020). Closer to variational classification, several works can be interpreted as treating softmax *inputs* as latent variables with a prior term to incorporate specific assumptions, e.g. encouraging *deterministic* label distributions (i.e. all probability mass on a single class) by imposing a *large margin* between class-conditional latent distributions (Liu et al., 2016; Wen et al., 2016; Wan et al., 2018; 2022; Scott et al., 2021).

Variational classification also relates to various works across learning paradigms in which a Gaussian mixture prior is imposed in the latent space, e.g. for representation learning (Xie et al., 2016; Caron et al., 2018), in auto-encoders (Song et al., 2013; Ghosh et al., 2019) and in variational auto-encoders (Jiang et al., 2016; Yang et al., 2017; Prasad et al., 2020; Manduchi et al., 2021).

5 Empirical Validation

Our goal is to empirically demonstrate that the latent structure induced by the VC objective is beneficial relative to that of a standard softmax classifier. A variational classifier can be used in place of any softmax classifier by making distributional choices appropriate for the data. Variational classification does not target any *one* of the known issues with softmax classifiers, rather to better reverse the generative process, which is expected to be of general benefit. We illustrate the effectiveness of a VC through a variety of tasks on familiar datasets in the visual and text domains. Specifically, we set out to validate the following hypotheses:

H1: The VC objective improves uncertainty estimation, leading to a more calibrated model.

H2: The VC objective increases model robustness to changes in the data distribution.

H3: The VC objective enhances resistance to adversarial perturbations.

H4: The VC objective aids learning from fewer samples.

For fair comparison, we make minimal changes to adapt a standard softmax classifier to a variational classifier. As described in §3.4, we train with the VC objective (Eqn. 7) under the following assumptions: $q_{\phi}(\mathbf{z}|x)$ is a delta distribution parameterised by a neural network encoder $f_{\omega}: \mathcal{X} \to \mathcal{Z}$; class-conditional priors $p_{\theta}(\mathbf{z}|y)$ are multi-variate Gaussians with parameters learned from the data (we use diagonal covariance for simplicity). To provide an ablation across the components of the VC objective, we compare classifiers trained to maximise three objective functions (see §3):

CE: equivalent to standard softmax cross-entropy under the above assumptions and corresponds to the MLE form of the VC objective (§3.2.1, (i)).

$$J_{\text{CE}} = \int_{x,y} p(x,y) \left\{ \int_{z} q_{\phi}(z|x) \log p_{\theta}(y|z) + \log p_{\pi}(y) \right\}$$

GM: includes class priors and corresponds to the MAP form of the VC objective (§3.2.1, (ii)). This is equivalent to Wan et al. (2018) with just the Gaussian prior.

$$J_{GM} = J_{CE} + \int_{x,y} p(x,y) \int_{z} q_{\phi}(z|y) \log p_{\theta}(z|y)$$

VC: includes the entropy of the empirical latent distributions and corresponds to the full (Bayesian form) VC objective (§3.2.1, (iii)).

$$J_{\text{VC}} = J_{\text{GM}} - \int_{x,y} p(x,y) \int_{z} q_{\phi}(z|y) \log q_{\phi}(z|y)$$

	CIFAR-10			CIFAR-100			Tiny-Imagenet				
	CE	GM^{\diamond}	VC	vMF^*	CE	GM *	VC	vMF^*	CE	GM^{\diamond}	VC
Acc. (%, ↑)											
WRN	96.2 ± 0.1	$95.0 \pm {\scriptstyle 0.2}$	$96.3 \pm {\scriptstyle 0.2}$	-	80.3 ± 0.1	$79.8 \pm {\scriptstyle 0.2}$	$80.3 \pm {\scriptstyle 0.1}$	-	-	-	-
RNET	93.7 ± 0.1	$93.0 \pm \scriptscriptstyle 0.1$	$93.2 \pm {\scriptstyle 0.1}$	$94.0 \pm \scriptscriptstyle 0.1$	73.2 ± 0.1	$74.2 {\scriptstyle~\pm~0.1}$	$73.4 \pm {\scriptstyle 0.1}$	$69.94 \pm {\scriptstyle 0.2}$	59.7 ± 0.2	$59.3 \pm {\scriptstyle 0.1}$	$59.3 \pm \scriptscriptstyle 0.1$
ECE (%, ↓)											
WRN	3.1 ± 0.2	$3.5~\pm~\text{0.3}$	$\textbf{2.1} \pm {\scriptstyle 0.2}$	-	11.1 ± 0.7	$19.6 \pm \scriptscriptstyle 0.4$	$\textbf{4.8}\pm{\scriptstyle 0.3}$	-	-	-	-
RNET	3.8 ± 0.3	$4.1{\scriptstyle~\pm~0.2}$	$\textbf{3.2} \pm {\scriptstyle 0.2}$	$5.9 \pm {\scriptstyle 0.2}$	8.7 ± 0.2	$10.5 \pm {\scriptstyle 0.2}$	$\textbf{5.1} \pm {\scriptstyle 0.2}$	$7.9 \pm {\scriptstyle 0.3}$	12.3 ± 0.4	$8.75~\pm~\scriptstyle 0.2$	$\textbf{7.4} \pm 0.5$

Table 1: Classification Accuracy and Expected Calibration Error (mean, std.dev. over 5 runs). Accuracy is comparable between VC and CE across encoder architectures and data sets, while calibration of VC notably improves. \star from Scott et al. (2021), \diamond our implementation of Wan et al. (2018)

5.1 Accuracy and Calibration

We first compare the classification accuracy and calibration of each model on three standard benchmarks (CIFAR-10, CIFAR-100, and TINY-IMAGENET), across two standard ResNet model architectures (WideResNet-28-10 (WRN) and ResNet-50 (RNET)) (He et al., 2016; Zagoruyko & Komodakis, 2016). Calibration is evaluated in terms of the Expected Calibration Error (ECE) (see Appendix C). Table 1 shows that the VC and GM models achieve comparable accuracy to softmax cross entropy (CE), but that the VC model is consistently, significantly more calibrated (H1). Unlike approaches such as Platt's scaling (Platt et al., 1999) and temperature scaling (Guo et al., 2017), no post hoc calibration is performed requiring additional data or associated hyperparameters tuning.

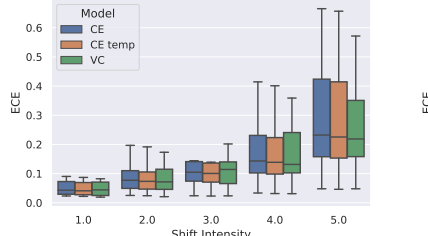
We also compare MC-Dropout (Gal & Ghahramani, 2016) for CIFAR-10 and CIFAR-100 on ResNet-50 (p = 0.2, averaging over 10 samples). As seen previously (Ovadia et al., 2019), although calibration improves relative to CE (3.3%, 1.4%, resp.), the main goal of classification, prediction accuracy, reduces (92.7%, 70.1%).

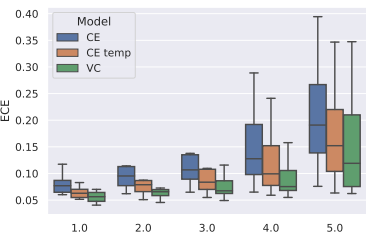
5.2 Generalization under distribution shift

When used in real-world settings, machine learning models may encounter distribution shift relative to the training data. It can be important to know when a model's output is reliable and can be trusted, requiring the model to be calibrated on out-of-distribution (OOD) data and know when they do not know. To test performance under distribution shift, we use the robustness benchmarks, CIFAR-10-C, CIFAR-100-C and Tiny-Imagenet-C, proposed by Hendrycks & Dietterich (2019), which simulate distribution shift by adding various synthetic corruptions of varying intensities to a dataset. We compare the CE model, with and without temperature scaling, to the VC model. Temperature scaling was performed as in Guo et al. (2017) with the temperature tuned on an in-distribution validation set.

Both models are found to perform comparably in terms of classification accuracy (Figure 8), according to previous results (§5.1). However, Figure 3 shows that the VC model has a consistently lower calibration error as the corruption intensity increases (left to right) (**H2**). We note that the improvement in calibration between the CE and VC models increases as the complexity of the dataset increases.

When deployed in the wild, *natural* distributional shifts may occur in the data due to subtle changes in the data generation process, e.g. a change of camera. We test resilience to *natural* distributional shifts on two tasks: Natural Language Inference (NLI) and detecting whether cells are cancerous from microscopic





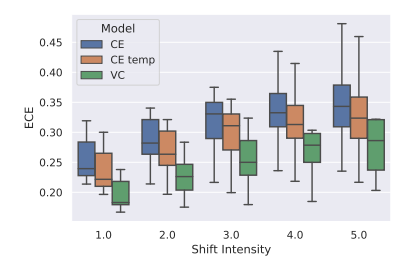


Figure 3: Calibration under distribution shift: (l) CIFAR-10-C, (m) CIFAR-100-C, (r) TINY-IMAGENET-C. Boxes indicate quartiles, whiskers indicate min/max, across 16 types of synthetic distribution shift.

images. NLI requires verifying if a hypothesis logically follows from a premise. Models are trained on the SNLI dataset (Bowman et al., 2015) and tested on the MNLI dataset (Williams et al., 2018) taken from more diverse sources. Cancer detection uses the Camelyon17 dataset (Bandi et al., 2018) from the WILDs datasets (Koh et al., 2021), where the train and eval sets contain images from different hospitals.

Table 2 shows that the VC model achieves better calibration under these natural distributional shifts (**H2**). The CAMELYON17 (CAM) dataset has a relatively small number (1000) of training samples (hence wide error bars are expected), which combines distribution shift with a low data setting (**H4**) and shows that the VC model achieves higher (average) accuracy in this more challenging real-world setting.

	Accura	acy (†)	Calibration (\downarrow)		
	CE	VC	$^{\mathrm{CE}}$	VC	
NLI	$\textbf{71.2} \pm 0.1$	$\textbf{71.2} \pm 0.1$	$7.3 \pm {\scriptstyle 0.2}$	3.4 ± 0.2	
CAM	79.2 ± 2.8	$\textbf{84.5} \pm 4.0$	$8.4 \pm {\scriptstyle 2.5}$	1.8 ± 1.3	

Table 2: Accuracy and Calibration (ECE) under distributional shift (mean, std. err., 5 runs)

We also test the ability to **detect OOD examples**. We compute the AUROC when a model is trained on CIFAR-10 and evaluated on the CIFAR-10 validation set mixed (in turn) with SVHN, CIFAR-100, and CELEBA (Goodfellow et al., 2013; Liu et al., 2015). We compare the VC and CE models using the probability of the predicted class $\arg\max_{y} p_{\theta}(y|x)$ as a means of identifying OOD samples.

Table 3 shows that the VC model performs comparably to the CE model. We also consider p(z) as a metric to detect OOD samples and achieve comparable results, which is broadly consistent with the findings of (Grathwohl et al., 2019). Although the VC model learns to map the data to a more structured latent space and, from the results above, makes more calibrated predictions for OOD data, it does not appear to be better able to distinguish OOD data than a standard softmax classifier (CE) using the metrics tested (we note that "OOD" is a loosely defined term).

Model	SVHN	C-100	CelebA
$P_{\text{CE}}(y x)$	0.92	0.88	0.90
$P_{\rm VC}(y z)$	0.93	0.86	0.89

Table 3: AUROC for OOD detection. Models trained on CIFAR-10, evaluated on in and out-of-distribution samples.

5.3 Adversarial Robustness

We test model robustness to adversarially generated images using the common Fast Gradient Sign Method (FGSM) of adversarial attack (Goodfellow et al., 2014b). This "attack" is arbitrarily chosen and VC is not explicitly tailored towards it. Perturbations are generated as $P = \epsilon \times sign(\nabla_x \mathcal{L}(x,y))$, where $\mathcal{L}(x,y)$ is the model loss for data sample x and correct class y; and ϵ is the attack magnitude. We compare all models trained on MNIST and CIFAR-10 against FGSM attacks of different magnitudes.

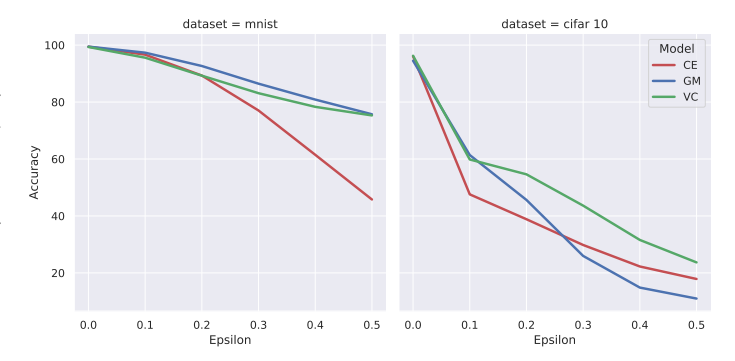


Figure 4: Prediction accuracy for increasing FGSM adversarial attacks (l) MNIST; (r) CIFAR-10

Results in Figure 4 show that the VC model is consistently more (FGSM) adversarially robust relative to the standard CE model, across attack magnitudes on both datasets (**H3**).

5.4 Low Data Regime

In many real-world settings, datasets may have relatively few data samples and it may be prohibitive or impossible to acquire more, e.g. historic data or rare medical cases. We investigate model performance when data is scarce on the hypothesis that a prior over the latent space enables the model to better generalise from fewer samples. Models are trained on 500 samples from MNIST, 1000 samples from CIFAR-10 and 50 samples from AGNEWS.

	CE	GM	VC
MNIST	93.1 ± 0.2	94.4 ± 0.1	94.2 ± 0.2
CIFAR-10	52.7 ± 0.5	54.2 ± 0.6	56.3 ± 0.6
AGNEWS	56.3 ± 5.3	61.5 \pm 2.9	$\textbf{66.3} \pm {\scriptstyle 4.6}$

Table 4: Accuracy in low data regime (mean, std.err., 5 runs)

Results in Table 4 show that introducing the prior (GM) improves performance in a low data regime and that the additional entropy term in the VC model maintains or further improves accuracy (H4), particularly on the more complex datasets.

We further probe the relative benefit of the VC model over the CE baseline as training sample size varies (**H4**) on 10 MedMNIST classification datasets (Yang et al., 2021), a collection of real-world medical datasets of varying sizes.

Figure 5 shows the increase in classification accuracy for the VC model relative to the CE model against number of training samples (log scale). The results show a clear trend that the benefit of the additional latent structure imposed in the VC model increases exponentially as the number of training samples decreases.

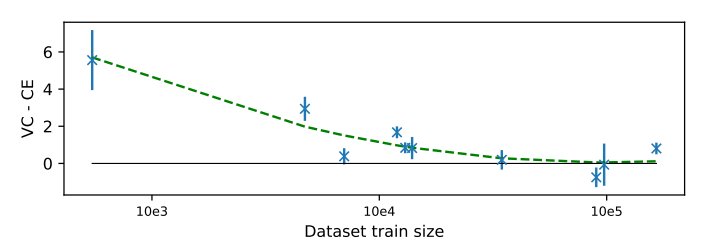


Figure 5: Accuracy increase of VC vs CE on 10 MedMNIST classification datasets of varying training set size. Blue points indicate accuracy on a dataset (mean, std.err., 3 runs). Green line shows a best-fit trend across dataset size.

Together with the results in Table 4, this suggests that the VC model offers most significant benefit for small, complex datasets.

6 Conclusion

We present Variational Classification (VC), a latent generalisation of standard softmax classification trained under cross-entropy loss, mirroring the relationship between the variational auto-encoder and the deterministic auto-encoder (§3). We show that softmax classification is a special case of VC under specific assumptions that are effectively taken for granted when using a softmax output layer. Moreover we see that latent distributional assumptions, "hard-coded" in the softmax layer and anticipated to be followed for accurate class predictions, are neither enforced theoretically nor satisfied empirically. We propose a novel training objective based on the ELBO to better align the *empirical* latent distribution to that *anticipated*. A series of experiments on image and text datasets show that, with marginal computational overhead and without tuning hyper-parameters other than for the original classification task, variational classification achieves comparable prediction accuracy to standard softmax classification while significantly improving calibration, adversarial robustness (specifically FGSM), robustness to distribution shift and performance in low data regimes.

In terms of limitations, we intentionally focus on the *output* layer of a classifier, treating the encoder f_{ω} as a "black-box". This leaves open question of how, and how well, the underlying neural network achieves its role of transforming a mixture of unknown data distributions p(x|y) to a mixture of specified latent distributions p(z|y). We also prove that optimal *empirical* latent distributions $q_{\phi}(z|y)$ are "peaky" approximations to the anticipated $p_{\theta}(z|y)$, leaving open the possibility of further improvement to the VC objective.

The VC framework gives new theoretical insight into the highly familiar softmax classifier, opening up several interesting future directions. For example, q(z|x) might be modelled by a stochastic distribution, rather than a delta distribution, to reflect uncertainty in the latent variables, similarly to a VAE. VC may also be extended to semi-supervised learning and related to approaches that impose structure in the latent space.

7 Acknowledgements

Carl is gratefully supported by an ETH AI Centre Postdoctoral Fellowships and a small projects grant from the Haslerstiftung (no. 23072). Mrinmaya acknowledges support from the Swiss National Science Foundation (Project No. 197155), a Responsible AI grant by the Haslerstiftung; and an ETH Grant (ETH-19 21-1).

References

- Kemal Adem, Serhat Kiliçarslan, and Onur Cömert. Classification and diagnosis of cervical cancer with stacked autoencoder and softmax classification. *Expert Systems with Applications*, 115:557–564, 2019.
- Carl Allen, Ivana Balažević, and Timothy Hospedales. A probabilistic model for discriminative and neuro-symbolic semi-supervised learning. arXiv preprint arXiv:2006.05896, 2020.
- Peter Bandi, Oscar Geessink, Quirine Manson, Marcory Van Dijk, Maschenka Balkenhol, Meyke Hermsen, Babak Ehteshami Bejnordi, Byungjae Lee, Kyunghyun Paeng, Aoxiao Zhong, et al. From detection of individual metastases to classification of lymph node status at the patient level: the camelyon17 challenge. In *IEEE Transactions on Medical Imaging*, 2018.
- Samuel R Bowman, Gabor Angeli, Christopher Potts, and Christopher D Manning. A large annotated corpus for learning natural language inference. arXiv preprint arXiv:1508.05326, 2015.
- Mathilde Caron, Piotr Bojanowski, Armand Joulin, and Matthijs Douze. Deep clustering for unsupervised learning of visual features. In *European Conference on Computer Vision*, 2018.
- Ting Chen, Simon Kornblith, Mohammad Norouzi, and Geoffrey Hinton. A simple framework for contrastive learning of visual representations. In *International Conference on Machine Learning*, 2020.
- Yarin Gal and Zoubin Ghahramani. Dropout as a bayesian approximation: Representing model uncertainty in deep learning. In *International Conference on Machine Learning*, 2016.
- Partha Ghosh, Mehdi SM Sajjadi, Antonio Vergari, Michael Black, and Bernhard Schölkopf. From variational to deterministic autoencoders. arXiv preprint arXiv:1903.12436, 2019.
- Ian J Goodfellow, Yaroslav Bulatov, Julian Ibarz, Sacha Arnoud, and Vinay Shet. Multi-digit number recognition from street view imagery using deep convolutional neural networks. arXiv preprint arXiv:1312.6082, 2013.
- Ian J Goodfellow, Jean Pouget-Abadie, Mehdi Mirza, Bing Xu, David Warde-Farley, Sherjil Ozair, Aaron C Courville, and Yoshua Bengio. Generative adversarial nets. In *Neural Information Processing Systems*, 2014a.
- Ian J Goodfellow, Jonathon Shlens, and Christian Szegedy. Explaining and harnessing adversarial examples. arXiv preprint arXiv:1412.6572, 2014b.
- Will Grathwohl, Kuan-Chieh Wang, Joern-Henrik Jacobsen, David Duvenaud, Mohammad Norouzi, and Kevin Swersky. Your classifier is secretly an energy based model and you should treat it like one. In *International Conference on Learning Representations*, 2019.
- Chuan Guo, Geoff Pleiss, Yu Sun, and Kilian Q Weinberger. On calibration of modern neural networks. In *International Conference on Machine Learning*, 2017.
- Michael Gutmann and Aapo Hyvärinen. Noise-contrastive estimation: A new estimation principle for unnormalized statistical models. In *International Conference on Artificial Intelligence and Statistics*, 2010.
- Kaiming He, Xiangyu Zhang, Shaoqing Ren, and Jian Sun. Deep residual learning for image recognition. In Conference on Computer Vision and Pattern Recognition, 2016.
- Dan Hendrycks and Thomas Dietterich. Benchmarking neural network robustness to common corruptions and perturbations. arXiv preprint arXiv:1903.12261, 2019.
- Zhuxi Jiang, Yin Zheng, Huachun Tan, Bangsheng Tang, and Hanning Zhou. Variational deep embedding: An unsupervised and generative approach to clustering. arXiv preprint arXiv:1611.05148, 2016.
- Diederik P Kingma and Max Welling. Auto-encoding variational bayes. In *International Conference on Learning Representations*, 2014.

- Marcus Klasson, Cheng Zhang, and Hedvig Kjellström. A hierarchical grocery store image dataset with visual and semantic labels. In *IEEE Winter Conference on Applications of Computer Vision*, 2019.
- Pang Wei Koh, Shiori Sagawa, Henrik Marklund, Sang Michael Xie, Marvin Zhang, Akshay Balsubramani, Weihua Hu, Michihiro Yasunaga, Richard Lanas Phillips, Irena Gao, et al. Wilds: A benchmark of in-the-wild distribution shifts. In *International Conference on Machine Learning*, 2021.
- Alex Krizhevsky, Ilya Sutskever, and Geoffrey E Hinton. Imagenet classification with deep convolutional neural networks. In *Neural Information Processing Systems*, 2012.
- Weiyang Liu, Yandong Wen, Zhiding Yu, and Meng Yang. Large-margin softmax loss for convolutional neural networks. In *International Conference on Machine Learning*, 2016.
- Ziwei Liu, Ping Luo, Xiaogang Wang, and Xiaoou Tang. Deep learning face attributes in the wild. In *International Conference on Computer Vision*, 2015.
- Alireza Makhzani, Jonathon Shlens, Navdeep Jaitly, Ian Goodfellow, and Brendan Frey. Adversarial autoencoders. arXiv preprint arXiv:1511.05644, 2015.
- Laura Manduchi, Kieran Chin-Cheong, Holger Michel, Sven Wellmann, and Julia Vogt. Deep conditional gaussian mixture model for constrained clustering. In *Neural Information Processing Systems*, 2021.
- Lars Mescheder, Sebastian Nowozin, and Andreas Geiger. Adversarial variational bayes: Unifying variational autoencoders and generative adversarial networks. In *International Conference on Machine Learning*, 2017.
- Milad Mirbabaie, Stefan Stieglitz, and Nicholas RJ Frick. Artificial intelligence in disease diagnostics: A critical review and classification on the current state of research guiding future direction. *Health and Technology*, 11(4):693–731, 2021.
- Jishnu Mukhoti, Andreas Kirsch, Joost van Amersfoort, Philip HS Torr, and Yarin Gal. Deep deterministic uncertainty: A simple baseline. arXiv e-prints, pp. arXiv-2102, 2021.
- Kevin P Murphy. Machine learning: a probabilistic perspective. MIT press, 2012.
- Mahdi Pakdaman Naeini, Gregory Cooper, and Milos Hauskrecht. Obtaining well calibrated probabilities using bayesian binning. In AAAI Conference on Artificial Intelligence, 2015.
- XuanLong Nguyen, Martin J Wainwright, and Michael I Jordan. Estimating divergence functionals and the likelihood ratio by convex risk minimization. *IEEE Transactions on Information Theory*, 56(11):5847–5861, 2010.
- Aaron van den Oord, Yazhe Li, and Oriol Vinyals. Representation learning with contrastive predictive coding. arXiv preprint arXiv:1807.03748, 2018.
- Yaniv Ovadia, Emily Fertig, Jie Ren, Zachary Nado, David Sculley, Sebastian Nowozin, Joshua Dillon, Balaji Lakshminarayanan, and Jasper Snoek. Can you trust your model's uncertainty? evaluating predictive uncertainty under dataset shift. In *Neural Information Processing Systems*, 2019.
- John Platt et al. Probabilistic outputs for support vector machines and comparisons to regularized likelihood methods. Advances in large margin classifiers, 10(3):61–74, 1999.
- Vignesh Prasad, Dipanjan Das, and Brojeshwar Bhowmick. Variational clustering: Leveraging variational autoencoders for image clustering. In *International Joint Conference on Neural Networks*, 2020.
- Danilo Jimenez Rezende, Shakir Mohamed, and Daan Wierstra. Stochastic backpropagation and approximate inference in deep generative models. In *International Conference on Machine Learning*, 2014.
- Tyler R Scott, Andrew C Gallagher, and Michael C Mozer. von mises-fisher loss: An exploration of embedding geometries for supervised learning. In *International Conference on Computer Vision*, 2021.

- Ravid Shwartz-Ziv and Naftali Tishby. Opening the black box of deep neural networks via information. arXiv preprint arXiv:1703.00810, 2017.
- Kihyuk Sohn, Honglak Lee, and Xinchen Yan. Learning structured output representation using deep conditional generative models. In *Neural Information Processing Systems*, 2015.
- Chunfeng Song, Feng Liu, Yongzhen Huang, Liang Wang, and Tieniu Tan. Auto-encoder based data clustering. In *Iberoamerican Congress on Pattern Recognition*, 2013.
- Charlie Tang and Russ R Salakhutdinov. Learning stochastic feedforward neural networks. In *Neural Information Processing Systems*, 2013.
- Jacob Tiensuu, Maja Linderholm, Sofia Dreborg, and Fredrik Örn. Detecting exoplanets with machine learning: A comparative study between convolutional neural networks and support vector machines, 2019.
- Naftali Tishby and Noga Zaslavsky. Deep learning and the information bottleneck principle. In *IEEE Information Theory Workshop*, 2015.
- Naftali Tishby, Fernando C Pereira, and William Bialek. The information bottleneck method. arXiv preprint physics/0004057, 2000.
- Ashish Vaswani, Noam Shazeer, Niki Parmar, Jakob Uszkoreit, Llion Jones, Aidan N Gomez, Łukasz Kaiser, and Illia Polosukhin. Attention is all you need. In *Neural Information Processing Systems*, 2017.
- Weitao Wan, Yuanyi Zhong, Tianpeng Li, and Jiansheng Chen. Rethinking feature distribution for loss functions in image classification. In *Conference on Computer Vision and Pattern Recognition*, 2018.
- Weitao Wan, Jiansheng Chen, Cheng Yu, Tong Wu, Yuanyi Zhong, and Ming-Hsuan Yang. Shaping deep feature space towards gaussian mixture for visual classification. In *IEEE Transactions on Pattern Analysis and Machine Intelligence*, 2022.
- Yandong Wen, Kaipeng Zhang, Zhifeng Li, and Yu Qiao. A discriminative feature learning approach for deep face recognition. In *European Conference on Computer Vision*, 2016.
- Adina Williams, Nikita Nangia, and Samuel Bowman. A broad-coverage challenge corpus for sentence understanding through inference. In *North American Chapter of the Association for Computational Linguistics: Human Language Technologies*, 2018.
- Junyuan Xie, Ross Girshick, and Ali Farhadi. Unsupervised deep embedding for clustering analysis. In *International Conference on Machine Learning*, 2016.
- Bo Yang, Xiao Fu, Nicholas D Sidiropoulos, and Mingyi Hong. Towards k-means-friendly spaces: Simultaneous deep learning and clustering. In *International Conference on Machine Learning*, 2017.
- Jiancheng Yang, Rui Shi, and Bingbing Ni. Medmnist classification decathlon: A lightweight automl benchmark for medical image analysis. In *International Symposium on Biomedical Imaging*, 2021.
- Sergey Zagoruyko and Nikos Komodakis. Wide residual networks. arXiv preprint arXiv:1605.07146, 2016.

A Proofs

A.1 Optimising the ELBO_{VC} w.r.t q

Rearranging Eqn. 5, the ELBO_{VC} is optimised by

$$\begin{split} & \operatorname*{arg\,max}_{q_{\phi}(z|x)} \int_{x} \sum_{y} p(x,y) \int_{z} q_{\phi}(z|x) \log p_{\theta}(y|z) \\ = & \operatorname*{arg\,max}_{q_{\phi}(z|x)} \int_{x} p(x) \int_{z} q_{\phi}(z|x) \sum_{y} p(y|x) \log p_{\theta}(y|z) \end{split}$$

The integral over z is a $q_{\phi}(z|x)$ -weighted sum of $\sum_{y} p(y|x) \log p_{\theta}(y|z)$ terms. Since $q_{\phi}(z|x)$ is a probability distribution, the integral is upper bounded by $\max_{z} \sum_{y} p(y|x) \log p_{\theta}(y|z)$. This maximum is attained iff support of $q_{\phi}(z|x)$ is restricted to $z^* = \arg \max_{z} \sum_{y} p(y|x) \log p_{\theta}(y|z)$ (which may not be unique).

A.2 Optimising the VC objective w.r.t. q

Setting $\beta = 1$ in Eqn. 7 to simplify and adding a lagrangian term to constrain $q_{\phi}(z|x)$ to a probability distribution, we aim to find

$$\begin{split} \underset{q_{\phi}(z|x)}{\arg\max} \int_{x} \sum_{y} p(x,y) \Big\{ \int_{z} q_{\phi}(z|x) \log p_{\theta}(y|z) \\ - \int_{z} q_{\phi}(z|y) \log \frac{q_{\phi}(z|y)}{p_{\theta}(z|y)} + \log p_{\pi}(y) \Big\} + \lambda (1 - \int_{z} q_{\phi}(z|x)) \ . \end{split}$$

Recalling that $q_{\phi}(z|y) = \int_{x} q_{\phi}(z|x)p(x|y)$ and using calculus of variations, we set the derivative of this functional w.r.t. $q_{\phi}(z|x)$ to zero

$$\sum_{y} p(x,y) \left\{ \log p_{\theta}(y|z) - \left(\log \frac{q_{\phi}(z|y)}{p_{\theta}(z|y)} + 1 \right) \right\} - \lambda = 0$$

Rearranging and diving through by p(x) gives

$$\mathbb{E}_{p(y|x)}[\log q_{\phi}(z|y)] = \mathbb{E}_{p(y|x)}[\log p_{\theta}(y|z)p_{\theta}(z|y)] + c ,$$

where $c = -(1 + \frac{\lambda}{p(x)})$. Further, if each label y occurs once with each x, due to sampling or otherwise, then this simplifies to

$$q_{\phi}(z|y^*)e^c = p_{\theta}(y^*|z)p_{\theta}(z|y^*)$$
,

which holds for all classes $y \in \mathcal{Y}$. Integrating over z shows $e^c = \int_z p_\theta(y|z) p_\theta(z|y)$ to give

$$q_{\phi}(z|y) = \frac{p_{\theta}(y|z)p_{\theta}(z|y)}{\int_{\mathbb{R}} p_{\theta}(y|z)p_{\theta}(z|y)} = p_{\theta}(z|y)\frac{p_{\theta}(y|z)}{\mathbb{E}_{p_{\theta}(z|y)}[p_{\theta}(y|z)]} \ . \qquad \Box$$

We note, it is straightforward to include β to show

$$q_{\boldsymbol{\phi}}(\boldsymbol{z}|\boldsymbol{y}) = p_{\boldsymbol{\theta}}(\boldsymbol{z}|\boldsymbol{y}) \frac{p_{\boldsymbol{\theta}}(\boldsymbol{y}|\boldsymbol{z})^{1/\beta}}{\mathbb{E}_{p_{\boldsymbol{\theta}}(\boldsymbol{z}|\boldsymbol{y})}[p_{\boldsymbol{\theta}}(\boldsymbol{y}|\boldsymbol{z})^{1/\beta}]}$$
 .

B Justifying the Latent Prior in Variational Classification

Choosing Gaussian class priors in Variational classification can be interpreted in two ways:

Well-specified generative model: Assume data $x \in \mathcal{X}$ is generated from the hierarchical model: $y \to z \to x$, where p(y) is categorical; p(z|y) are analytically known distributions, e.g. $\mathcal{N}(z; \mu_y, \Sigma_y)$; the dimensionality of z is not large; and x = h(z) for an arbitrary invertible function $h : \mathcal{Z} \to \mathcal{X}$ (if \mathcal{X} is of higher dimension than \mathcal{Z} , assume h maps one-to-one to a manifold in \mathcal{X}). Accordingly, p(x) is a mixture of unknown distributions. If $\{p_{\theta}(z|y)\}_{\theta}$ includes the true distribution p(z|y), variational classification effectively aims to invert h and learn the parameters of the true generative model. In practice, the model parameters and h^{-1} may only be identifiable up to some equivalence, but by reflecting the true latent variables, the learned latent variables should be semantically meaningful.

Miss-specified model: Assume data is generated as above, but with z having a large, potentially uncountable, dimension with complex dependencies, e.g. details of every blade of grass or strand of hair in an image. In general, it is impossible to learn all such latent variables with a lower dimensional model. The latent variables of a VC might learn a complex function of multiple true latent variables.

The first scenario is ideal since the model might learn disentangled, semantically meaningful features of the data. However, it requires distributions to be well-specified and a low number of true latent variables. For natural data with many latent variables, the second case seems more plausible but choosing $p_{\theta}(\mathbf{z}|y)$ to be Gaussian may nevertheless be justifiable by the Central Limit Theorem.

C Calibration Metrics

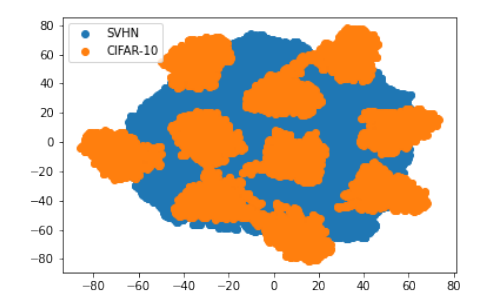
One way to measure if a model is calibrated is to compute the expected difference between the confidence and expected accuracy of a model.

$$\mathbb{E}_{P(\hat{y}|x)} \left[\mathbb{P}(\hat{y} = y | P(\hat{y}|x) = p) - p \right]$$
(12)

This is known as expected calibration error (ECE) (Naeini et al., 2015). Practically, ECE is estimated by sorting the predictions by their confidence scores, partitioning the predictions in M equally spaced bins $(B_1
ldots B_M)$ and taking the weighted average of the difference between the average accuracy and average confidence of the bins. In our experiments we use 20 equally spaced bins.

$$ECE = \sum_{m=1}^{M} \frac{|B_m|}{n} |acc(B_m) - conf(B_m)|$$
(13)

D OOD Detection



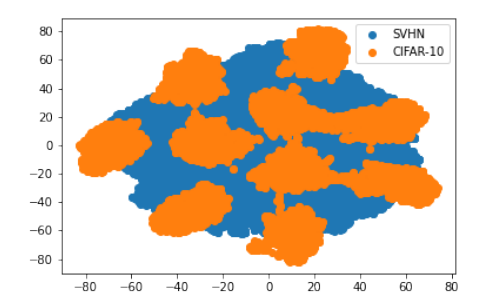


Figure 6: t-SNE plots of the feature space for a classifier trained on CIFAR-10. (l) Trained using CE. (r) Trained using VC. We posit that similar to CE, VC model is unable to meaningfully represent data from an entirely different distribution.

E Semantics of the latent space

To try to understand the semantics captured in the latent space, we use a pre-trained MNIST model on the *Ambiguous MNIST* dataset (Mukhoti et al., 2021). We interpolate between ambiguous 7's that are mapped close to the Gaussian clusters of classes of "1" and "2". It can be observed that traversing from the mean of the "7" Gaussian to that of the "1" class, the ambiguous 7's begin to look more like "1"s.

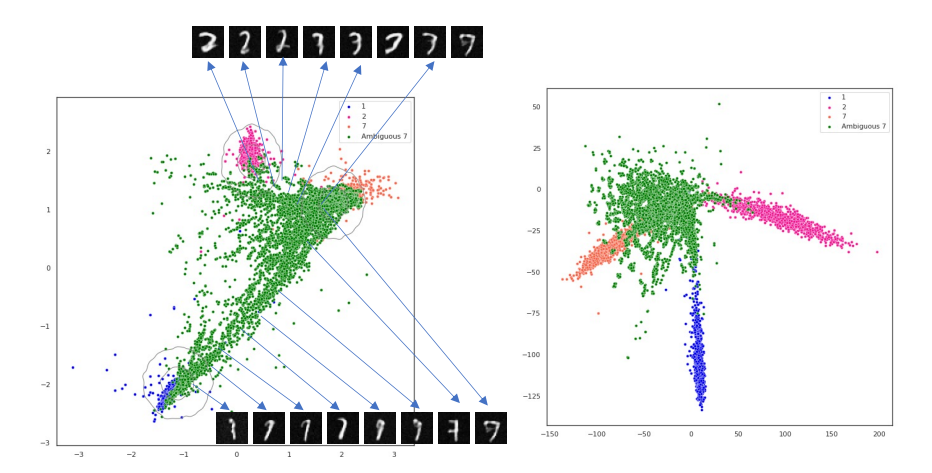


Figure 7: Interpolating in the latent space: Ambiguous MNIST when mapped on the latent space. (l) VC, (r) CE

F Classification under Domain Shift

A comparison of accuracy between the VC and CE models under 16 different synthetic domain shifts. We find that VC performs comparably well as CE.

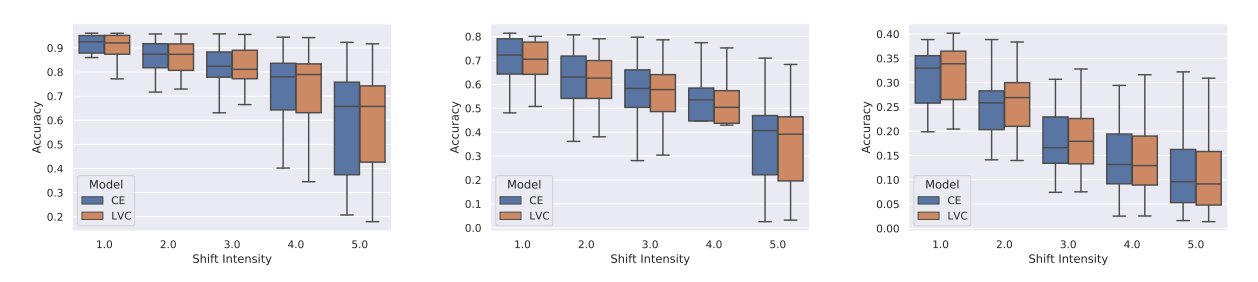


Figure 8: Classification accuracy under distributional shift: (left) CIFAR-10-C (middle) CIFAR-100-C (right) TINY-IMAGENET-C